Atmos. Chem. Phys. Discuss., 13, 14749–14795, 2013
www.atmos-chem-phys-discuss.net/13/14749/2013/
doi:10.5194/acpd-13-14749-2013

Atmospheric Chemistry and Physics
Discussions
Open Access

This discussion paper is/has been under review for the journal Atmospheric Chemistry and Physics (ACP). Please refer to the corresponding final paper in ACP if available.

Optimizing Saharan dust CALIPSO retrievals

V. Amiridis[1], U. Wandinger[2], E. Marinou[1], E. Giannakaki[3], A. Tsekeri[1], S. Basart[4], S. Kazadzis[5], A. Gkikas[1,6], M. Taylor[5], J. Baldasano[4,7], and A. Ansmann[2]

[1]Institute for Astronomy, Astrophysics, Space Applications and Remote Sensing, National Observatory of Athens, Athens, 15236, Greece
[2]Leibniz Institute for Tropospheric Research (TROPOS), Leipzig, Germany
[3]Finnish Meteorological Institute, Kuopio Unit, Finland
[4]Barcelona Supercomputing Center, Barcelona, Spain
[5]Institute of Environmental Research and Sustainable Development, National Observatory of Athens, Greece
[6]Laboratory of Meteorology, Department of Physics, University of Ioannina, Greece
[7]Environmental Modelling Laboratory, Technical University of Catalonia, Barcelona, Spain

Received: 25 April 2013 – Accepted: 21 May 2013 – Published: 5 June 2013

Correspondence to: V. Amiridis (vamoir@noa.gr)

Published by Copernicus Publications on behalf of the European Geosciences Union.

Abstract

We demonstrate improvements in CALIPSO dust extinction retrievals over North Africa and Europe when corrections are applied regarding the Saharan dust lidar ratio assumption, the separation of dust portion in detected dust mixtures, and the averaging scheme introduced in the Level 3 CALIPSO product. First, a universal, spatially constant lidar ratio of 58 sr instead of 40 sr is applied to individual Level 2 dust-related backscatter products. The resulting aerosol optical depths show an improvement compared with synchronous and co-located AERONET measurements. An absolute bias of the order of −0.03 has been found, improving on the statistically significant biases of the order of −0.10 reported in the literature for the original CALIPSO product. When compared with the MODIS co-located AOD product, the CALIPSO negative bias is even less for the lidar ratio of 58 sr. After introducing the new lidar ratio for the domain studied, we examine potential improvements to the climatological CALIPSO Level 3 extinction product: (1) by introducing a new methodology for the calculation of pure dust extinction from dust mixtures and (2) by applying an averaging scheme that includes zero extinction values for the non-dust aerosol types detected. The scheme is applied at a horizontal spatial resolution of 1° × 1° for ease of comparison with the instantaneous and co-located dust extinction profiles simulated by the BSC-DREAM8b dust model. Comparisons show that the extinction profiles retrieved with the proposed methodology reproduce the well-known model biases per sub-region examined. The very good agreement of the proposed CALIPSO extinction product with respect to AERONET, MODIS and the BSC-DREAM8b dust model, makes this dataset an ideal candidate for the provision of an accurate and robust multi-year dust climatology over North Africa and Europe.

1 Introduction

Since the launch of the Cloud-Aerosol Lidar with Orthogonal Polarization (CALIOP) instrument on board the Cloud-Aerosol Lidar and Infrared Pathfinder Satellite Observations (CALIPSO; Winker et al., 2009) satellite in June 2006, global aerosol and cloud profiles are provided to the scientific community through analysis of CALIOP backscatter observations at the operating wavelengths of 532 and 1064 nm. CALIOP probes the atmospheric vertical structure which is geometrically separated in layers (Vaughan et al., 2009) with each layer being characterized either as cloud or aerosol (Liu et al., 2009). For aerosol observations, a further discrimination into six subtypes (dust, marine, smoke, polluted dust, polluted continental and clean continental) is performed based on the layer-integrated attenuated backscatter and approximate particulate depolarization ratio, as well as the location of the measurement (either land or ocean; Omar et al., 2009). Based on the aerosol classification scheme, CALIPSO algorithms produce aerosol extinction and backscatter coefficients using a look-up table for the six aerosol types in order to define the aerosol-type-dependent Lidar Ratio (LR), a parameter that is required for the inversion of Level 1 attenuated backscatter coefficient profiles. The LRs are estimated from scattering calculations based on the definition of typical size distributions and refractive indexes for each aerosol type, mostly drawn from analysis of global Aerosol Robotic Network (AERONET) observations (Omar et al., 2009).

Following the retrieval of extinction coefficient profiles, the Aerosol Optical Depth (AOD) for each CALIPSO layer is obtained by integrating with respect to height. Validation studies performed so far in order to evaluate columnar CALIPSO estimates of AOD, have revealed low biases with respect to other global observations (e.g., Kittaka et al., 2011; Redemann et al., 2012; Schuster et al., 2012; Ma et al., 2012). With regard to the Moderate Resolution Imaging Spectroradiometer (MODIS) sensor, most studies emphasize a CALIPSO under-estimation of the order of 0.1 over regions having a strong mineral dust presence like the Mediterranean (Kittaka et al., 2011; Redemann et al., 2012). However, MODIS AOD accuracy decreases with cloud cover (e.g., Loeb and Smith, 2005; Zhang and Reid, 2006), and a detailed evaluation of CALIPSO products using other data sources is needed for conclusive comparisons. Recently, Schuster et al. (2012) compared CALIPSO AODs with AERONET and found that the relative bias of CALIPSO with respect to 147 global sun-photometric stations is −13 % when dust is present and −3 % when dust retrievals are not included in the analysis. The results reported in this study are based on the segregation of the dataset for different aerosol types based on the CALIPSO aerosol classification. Although this aerosol classification scheme is yet to be thoroughly evaluated (e.g. Burton et al., 2013), the CALIOP depolarization sensor has proven to be a direct and robust means by which mineral dust can be identified (e.g., Omar et al., 2009) and thus the results reported in Schuster et al. (2012) are likely to be representative for this aerosol type.

In any case, a detailed evaluation of CALIPSO dust extinction profiles (rather than AODs) using ground-based Raman lidars would be the ideal way to evaluate the reported CALIPSO under-estimations for dust and to investigate possible causes of such discrepancies. So far, only a small number of Level 2 CALIPSO evaluations using Raman lidars have been reported in the literature (e.g., Pappalardo et al., 2010). Most evaluation studies have been performed over Europe in the framework of the European Aerosol Research Lidar Network (EARLINET) and over North America using High Spectral Resolution Lidar (HSRL) airborne measurements during CALIPSO under-flights of the NASA B200 aircraft (e.g. Kacenelenbogen et al., 2011; Burton et al., 2013), i.e. at sites having complex aerosol mixtures that are not suitable for pure dust detection and therefore validation. It is only recently that Tesche et al. (2013) utilized ground-based Raman lidar measurements over Cape Verde, performed during the second Saharan Mineral Dust Experiment (SAMUM), in order to validate CALIPSO pure dust observations. The researchers reported an under-estimation of the CALIPSO Level 2 product for the 532 nm extinction coefficient as high as 30 % and attributed the difference to the low dust LR value of 40 sr used in the CALIPSO algorithm at this wavelength.

ACPD
13, 14749–14795, 2013

The LR value of 40 sr has been estimated by assuming typical size distributions and refractive indexes obtained from AERONET dust sites and then applying scattering calculations using the discrete dipole approximation technique to account for non-spherical particles (Omar et al., 2009). This value has also been retrieved directly from CALIPSO observations of isolated dust layers. In particular, AOD constraints have been set for dust layers (Liu et al., 2008) allowing LRs to be retrieved. Liu et al. (2008) report an effective dust LR of the order of 41 ± 6 sr at various locations in the Saharan dust plume off the west coast of Africa, agreeing well with the dust model of Omar et al. (2009).

Although CALIPSO dust retrievals may appear to be self-consistent, comparisons with ground-based Raman lidar measurements of Saharan dust show considerable discrepancies with respect to the LR at 532 nm. Direct LR measurements of pure Saharan dust obtained by the SAMUM-1 experiment, yield LRs of 55 ± 7 sr at 532 nm (Tesche et al., 2009a). Moreover, EARLINET reports a broad range of dust LRs from 30 sr to 80 sr across Europe (e.g., Mattis et al., 2002; Balis et al., 2004; Mona et al., 2006; Papayannis et al., 2008). This large dispersion in EARLINET LRs is mostly attributed to variations in the mixing of dust with other aerosol types, since the values are retrieved from the analysis of Raman lidar measurements during Saharan dust advection over the lidar sites, being contaminated by the presence of local aerosol sources. The statistical analysis presented in this paper is based on the separation of elevated layers of pure dust in EARLINET observations and reveals LRs at 532 nm equal to 58 ± 8 sr. This value is also supported by recent AERONET calculations performed by Schuster et al. (2012) using a different methodology to that of Omar et al. (2009). The highest LRs obtained by Schuster et al. (2012) of the order of 58 sr occurred at sites in Africa that are not located in the Sahel while the lowest LRs of the order of 43 sr were found in the Middle East. Schuster et al. (2012) attributed the variability in the retrieved LR to the variability of the real refractive index of dust, which in turn, is caused by the variability of the relative proportion of the mineral illite.

ACPD
13, 14749–14795, 2013

An explanation for the difference between the LR of 58 sr that is closer to all reported values from SAMUM-1, EARLINET and Schuster et al. (2012), and the LR of 40 sr used in the CALIPSO retrieval algorithm has been provided in detail in Wandinger et al., (2010). This latter study showed that the 40 sr value used by CALIPSO is an effective LR accounting for the increased atmospheric transmission caused by multiple scattering, and gives reasonable backscatter coefficients that compare well with ground-based observations. However, using the same value of 40 sr to convert backscatter into extinction coefficients, introduces a systematic under-estimation of extinction and AOD by 25–35 % (Wandinger et al., 2010; Tesche et al., 2013). The authors suggest that this artifact can easily be overcome by applying two different look-up values for the LR of mineral dust in the CALIPSO retrieval algorithm, i.e., an effective value of 40 sr for the backscatter retrieval and a single-scattering value of 55 sr for the backscatter-to-extinction conversion. In addition, the authors suggest that CALIPSO dust retrievals could be further optimized by applying the method introduced by Tesche et al. (2009b) for separating out the dust portion of the polluted dust CALIPSO aerosol type.

In this work, we investigate the possible improvement of CALIPSO dust retrievals by applying the LR value of 58 sr to CALIPSO backscatter retrievals. Moreover, we examine potential improvements on climatological monthly means when accounting for pure dust only, by separating pure dust from both “polluted dust” and “dust” CALIPSO subtypes. The domain of our application is North Africa and Europe, and we wish to note that this methodology cannot be applied to mineral dusts different from those advected from the Sahara desert. This point has been re-emphasized by the recent study of Schuster et al. (2012) which implied that the use of a spatially constant LR for all CALIPSO dust retrievals is inappropriate and would produce positive bias for CALIPSO AODs over the Middle East where the dust LR is lower than that for Sahara (of the order of 43 sr). The data used in this study refer to a domain that excludes the Middle East, and are presented in Sect. 2. Methodologies followed for each comparison together with the corresponding results are presented in Sect. 3, and the paper closes with our conclusions in Sect. 4.

ACPD
13, 14749–14795, 2013

2 Data

Satellite and ground-based observations with their corresponding products and the dust model utilized for Saharan dust simulations used in this study are described in this section.

2.1 The CALIPSO product

CALIOP, the principal instrument on board the CALIPSO satellite of the NASA A-Train, is a standard dual-wavelength (532 and 1064 nm) backscatter lidar operating a polarization channel at 532 nm (Winker et al., 2009), and has been acquiring global atmospheric profiles since June 2006. CALIOP measures high-resolution (1/3 km in the horizontal direction and 30 m in the vertical direction) profiles of the attenuated backscatter of aerosols and clouds at 532 and 1064 nm along with polarized backscatter in the visible channel (Winker et al., 2009). This data is distributed as part of CALIPSO Level 1 products. After calibration and range correction, cloud and aerosol layers are identified and aerosol backscatter and extinction are retrieved at 532 nm and 1064 nm and delivered in the Level 2 product. In this study, we use the CALIOP Level 2 product which is derived from the Level 1 product using a succession of algorithms that are described in detail in a special issue of the Journal of Atmospheric and Oceanic Technology (e.g., Winker et al., 2009). In brief, the CALIOP Level 2 retrieval scheme is composed of an algorithm for feature detection, a module that classifies features according to layer type (e.g., aerosol vs. cloud) and sub-type, and finally, an extinction retrieval algorithm that estimates the aerosol backscatter and extinction coefficient profile and total column aerosol optical depth (AOD) for an assumed LR for each detected aerosol layer. The CALIPSO Level 2 product determines the locations of layers within the atmosphere (Vaughan et al., 2009), discriminates aerosol layers from clouds (Liu et al., 2009), categorizes aerosol layers as one of six subtypes (dust, marine, smoke, polluted dust, polluted continental, and clean continental; Omar et al., 2009), and estimates the AOD of each layer detected (Young and Vaughan, 2009). Due to CALIOP's sensitivity to po-

ACPD
13, 14749–14795, 2013

larization at 532 nm, the depolarization arising from scattering from non-spherical dust particles serves as an independent means of discrimination between dust and other aerosol species.

In this study we use Version 3.01 of the Level 2 product. The older Version 2 product reported aerosol spatial properties (in the layer product files) at a horizontal resolution of 5 km, and range-resolved aerosol optical properties (in the profile product files) at a horizontal resolution of 40 km. The new Version 3 data products report aerosol optical properties at the same 5 km horizontal resolution used for the spatial properties. However, the same optical properties retrieval strategy is used in both Versions 2 and 3 of the CALIOP data products (Young and Vaughan, 2009).

Moreover, we use the methodology developed for the production of the Level 3 aerosol product (Winker et al., 2013), in order to derive $1^\circ \times 1^\circ$ latitude–longitude monthly-averaged vertical distributions. This methodology has been developed in order to produce the CALIPSO Level 3 product, in which the Level 2 532 nm aerosol extinction product is aggregated onto a global $2^\circ \times 5^\circ$ latitude–longitude grid. The vertical resolution of the product is 60 m over the range of heights −0.5 to 12 km relative to the mean sea level. Mean extinction profiles are computed for dust-only and for all aerosol types. CALIOP retrieves aerosol below optically thin cloud, in clear skies and above clouds. Monthly-mean extinction profiles are computed for four conditions: daytime: all-sky and cloud-free, and nighttime: all-sky and cloud-free. In addition, several quality control flags contained in the Level 2 files are used to screen the data prior to averaging. A detailed summary of the methodology used for the production of the Level 3 product is provided in the Appendix found at Winker et al. (2013).

2.2 The AERONET product

Ground-based AOD measurements from the well-known AEerosol RObotic NETwork (AERONET) of NASA (Holben et al., 2001) are used for validation purposes in our study. AERONET sun-photometers provide directly measured AODs at seven wavelengths from UV to the near-IR (approximately 0.340, 0.380, 0.440, 0.500, 0.675, 0.870,

ACPD
13, 14749–14795, 2013

and 1.02 µm) with an estimated uncertainty of 0.01–0.02 (Holben et al., 2001). In the present study, quality-assured direct-sun data (Level 2, Version 2) in the wavelength range 440–870 nm is used.

2.3 The MODIS product

Level 3 gridded daily mean AODs at 550 nm from the MODIS on board the Aqua satellite are utilized in our study. Our selection of MODIS-Aqua rather than MODIS on board the Terra satellite is based to the fact that CALIPSO is flown in formation with Aqua as part of the A-train satellite constellation, so that a large number of co-incident observations are available from the CALIOP and MODIS-Aqua instruments. A detailed description of the MODIS aerosol product is given in for example Remer et al. (2002) and the accuracy of MODIS AODs has been evaluated against ground measurements globally (e.g., Levy et al., 2010). Over sea surfaces, the accuracy of the AOD is $\pm 0.03 \pm 0.05 * \text{AOD}$ and is higher than that over vegetated land $\pm 0.05 \pm 0.2 * \text{AOD}$ (Ichoku et al., 2002; Remer et al., 2005). Over land, errors larger than $\pm 0.05 \pm 0.2 * \text{AOD}$ can be found in coastal zones due to sub-pixel water contamination (Barnaba and Gobbi, 2004).

In this study, we use Level 3 $1^\circ \times 1^\circ$ gridded daily mean values of the AOD at 550 nm from Collection 5.1. In addition, we use information on the Level 2 counts used for the production of the Level 3 AOD in order to constrain our dataset to representative $1^\circ \times 1^\circ$ Level 3 values, calculated by an adequate number of 10 km × 10 km Level 2 records. Deep Blue retrievals (Hsu et al., 2004) over bright surfaces such as deserts are ignored, since no information on the number of Level 2 cells used for the derivation of the Deep Blue Level 3 product is provided in the current version. Moreover, we utilize the total cloud coverage product in order to constrain our datasets to retrievals under almost cloud-free conditions, since the presence of clouds is a determining factor that strongly affects the accuracy of the algorithm retrieval and usually leads to a significant over-estimation of the AOD (e.g. Zhang et al., 2005; Remer et al., 2008).

ACPD
13, 14749–14795, 2013

2.4 The BSC-DREAM8b dust model

Dust extinction and dust AOD at 550 nm simulated by the BSC-DREAM8b dust model are utilized in this work to compare with the CALIPSO Level 3 dust product in the domain of interest. BSC-DREAM8b (Nickovic et al., 2001; Pérez et al., 2006a,b) is a regional model designed to simulate and predict the atmospheric cycle of mineral dust aerosol. The model is fully embedded as one of the governing prognostic equations in the atmospheric NCEP/Eta model and it solves the mass balance equation for dust taking into account the following processes: (1) dust production scheme (Shao et al., 1993) including a viscous sub-layer (Janjic, 1994), (2) horizontal and vertical advection, (3) turbulent and lateral diffusion (Janjic, 1994), (4) dry deposition and gravitational settling (Zhang et al., 2001), and (5) a simple below-cloud scavenging scheme (Nickovic et al., 2001). The model includes a source function based on the arid and semi-arid categories of the 1 km land-use data set provided by the US Geological Survey (USGS), eight size bins within the 0.1–10 µm radius range according to Tegen and Lacis (1996), a source size distribution derived from D'Almeida (1987), as well as dust radiative feedbacks on meteorology (Pérez et al., 2006a).

In recent years, operational versions of the model have been used for dust forecasting and as a dust research tool in North Africa and southern Europe (e.g., Pay et al., 2010; Kokkalis et al., 2012). Several case studies have highlighted the high capability of BSC-DREAM8b (e.g., Pérez et al., 2006a,b; Amiridis et al., 2009) with regard to both the horizontal and vertical extent of dust plumes in the Mediterranean Basin. The model has also been validated and tested over longer time periods in Europe (e.g., Basart et al., 2012) and against measurements in source regions during the SAMUM-1 (Haustein et al., 2009) and the Bodélé Dust Experiments (BoDEx; Todd et al., 2008). Additionally, in order to improve the dust forecast and to implement operational products, daily evaluation with near-real-time (NRT) observations is conducted at the Barcelona Supercomputer Center (BSC) in collaboration with the Spanish Meteorological State Agency (AEMET). Currently, the NRT evaluation includes both satellites (MODIS and Meteosat) and AERONET sunphotometers.

The initial state of the dust concentration in the BSC-DREAM8b model is defined by the 24 h forecast from the previous-day model run. For the present study, global meteorological files (at $1^\circ \times 1^\circ$) at 00:00 UTC from the National Center for Environmental Prediction's Global Forecast System (FNL/NCEP) are used as initial conditions and boundary conditions at intervals of 6 h. The resolution is set to 1/3 degree in the horizontal and to 24 layers extending up to approximately 15 km in the vertical. The domain of simulation covers northern Africa, the Mediterranean Sea, southern Europe and the Middle East. The output of model simulations is available hourly. The model outputs have been re-gridded to a horizontal resolution of $1^\circ \times 1^\circ$ so as to be suitable for the present analysis.

In BSC-DREAM8b, the AOD ($\tau(\lambda)$) and the extinction coefficient ($\alpha(\lambda)$) are related to column mass loading and mass concentration, respectively by:

$$\tau(\lambda) = \sum_{k=1}^{8} \tau_k(\lambda) = \sum_{k=1}^{8} \frac{3}{4\rho_k r_k} M_k Q_{\text{ext}}(\lambda)_k \tag{1}$$

$$a(\lambda) = \sum_{k=1}^{8} a_k(\lambda) = \sum_{k=1}^{8} \frac{3}{4\rho_k r_k} C_k Q_{\text{ext}}(\lambda)_k \tag{2}$$

where for each size bin k: $\tau_k(\lambda)$ is the aerosol optical depth, $\alpha_k(\lambda)$ is the extinction coefficient, ρ_k is the particle mass density, r_k is the effective radius, M_k is the column mass loading, C_k is the concentration, and $Q_{\text{ext}}(\lambda)_k$ is the extinction efficiency factor calculated using Mie scattering theory.

ACPD
13, 14749–14795, 2013

Title Page
Abstract | Introduction
Conclusions | References
Tables | Figures
◀◀ | ▶▶
◀ | ▶
Back | Close
Full Screen / Esc
Printer-friendly Version
Interactive Discussion

3 Methods, results and discussion

3.1 CALIPSO comparison with AERONET

3.1.1 Comparison methodology

In order to compare CALIPSO dust AODs with AERONET measurements for the 5 yr period between 2007 and 2011 of our analysis, we apply the method introduced by Schuster et al. (2012) to spatially co-locate and synchronize CALIPSO and AERONET data. The spatial co-location is based on an acceptable closest approach between the CALIPSO overpass and AERONET station, determined to be equal to 80 km. The time synchronization of the observations is defined as a 30 min difference of the CALIPSO closest-approach to a single AERONET AOD measurement. The use of the AERONET Level 2 quality-assured product ensures the lowest possible contamination of the AOD measurement by clouds. In order to convert AERONET AODs to the CALIOP operating wavelength of 532 nm, the methodology introduced by Schuster et al. (2006) is applied. CALIPSO AODs are produced from the integration with respect to height of the 5 km extinction coefficient profiles provided in Version 3 of Level 2 product. Only profiles with pure dust presence in the atmospheric column are accepted. Since our intention is to use only cloud-free profiles, it was a requirement that the CALIPSO cloud and aerosol detection (CAD) score for these profiles was lower than −20. Moreover, we required that the Extinction Quality control (QC) flag was equal to zero, indicating that a successful extinction solution was achieved with the default LR assigned to each layer. Finally, we required that CALIPSO surface elevations were within 100 m from the AERONET site in order to ensure that the optical path lengths for the CALIPSO and AERONET instruments were approximately equal. The locations used in this study were restricted to the domain of latitudes between 20 and 55 degrees and longitudes between −20 and 30 degrees. As a result, 11 AERONET stations fulfilled the aforementioned requirements: Dakar, Caceres, Autilla, Chilbolton, Le Fauga, Dunkerque, Venise, Gustav Dalen Tower, FORTH CRETE, Toravere and Eforie. The locations of

ACPD
13, 14749–14795, 2013

the AERONET stations used in our study can be found at the AERONET website (http://aeronet.gsfc.nasa.gov/).

3.1.2 Results and discussion

Considering atmospheres where CALIPSO detects only dust in the atmospheric column, we found 103 satellite overpasses with a distance less or equal to 80 km from the reference AERONET stations located in the domain of our interest. A significant absolute bias (average CALIPSO AOD minus the average AERONET AOD) of the order of −0.1 is revealed by our dataset. This absolute bias, found for Saharan dust, is almost identical with that reported by Schuster et al. (2012) for dust worldwide. Both absolute biases with respective 67 % and 95 % confidence intervals are shown in Fig. 1 (upper panel), and detailed statistics for our comparison is presented in Table 1. In general, we find good agreement with Schuster et al. (2012) for both the absolute biases and all the statistical parameters of Table 1 (e.g., relative biases of the order of −0.37 and large RMS biases of the order of 0.12). As already stated in Schuster et al. (2012), the high correlations and large relative biases of the dust comparisons in their work (but also here) indicate that dust aerosols are generally being "typed" correctly over the AERONET sites, but that perhaps the LR assigned to dust is too low. Thus, the LR under-estimation is believed to be the main factor affecting the CALIOP AOD under-estimation, and is expected to be linearly higher for higher AODs. The expected linear increase with AOD is revealed here if we separate the 5 km CALIPSO absolute biases by AOD class (Fig. 1 – lower panel). While absolute biases are affected more by larger AODs, relative biases with respect to AOD class consistently show a random variability around a −33 % average (Fig. 1 – lower panel), which is what is expected when underestimating LR. Backscatter errors on the other hand, do not diverge so much with the LR assumption for an elastic lidar. For example, Tesche et al. (2013) in a study using 15 co-located/synchronous ground-based lidar measurements during CALIPSO overpasses, showed that CALIPSO retrievals work best for the 532 nm backscatter coefficient. However, for dust cases it was found that using the effective dust LR of 40 sr

Discussion Paper | Discussion Paper | Discussion Paper | Discussion Paper |

ACPD

13, 14749–14795, 2013

Optimizing Saharan dust CALIPSO retrievals

V. Amiridis et al.

for the retrieval rather than the observed mean LR value of 55 sr in their dataset, led to an under-estimation of the 532 nm extinction coefficient by as much as 30 %. When the backscatter values were corrected for the low LR (i.e., by multiplying the backscatter by the ratio 55/40), the agreement between ground-based and CALIPSO extinctions was significantly improved.

Here, we follow the same approach in order to investigate this potential improvement on our CALIPSO–AERONET comparison. We use the 532 nm backscatter coefficient retrievals of CALIPSO multiplied by the value 58/40. The mean LR of 58 sr is the value that we derive by processing multi-year EARLINET Raman lidar measurements of pure Saharan dust. To be more specific, this LR has been retrieved by in-depth investigation of more than 500 aerosol layers selected from measured dust profiles at 16 EARLINET stations. Layer boundaries have been determined by the application of the derivative method (e.g., Mattis et al., 2008) and for each layer analyzed, mean optical properties have been retrieved, and the BSC-DREAM8b dust model has been used in order to validate the dust origin of each dust layer. The analysis of the EARLINET observed dust layers revealed statistical average LR values of 58 ± 9 sr at 532 nm and 58 ± 11 sr at 355 nm, showing almost no wavelength dependence for this parameter. As mentioned earlier, these values are consistent with measured LRs over the Saharan desert during the SAMUM-1 experiment (e.g., Tesche et al., 2009b).

Following the same co-location methodology as Tesche et al. (2013), the AOD retrievals from CALIPSO and AERONET using average LR values of 40 sr and 58 sr are compared in the scatter plots presented in the upper panel of Fig. 2. To the left, the original CALIPSO 5 km AOD retrieval taken from the integration of Level 2 extinction coefficient profiles is compared, while to the right, the same comparison is presented with the LR adjusted to 58 sr. The comparison is clearly improved, showing however a large AOD variability for some CALIPSO overpasses, indicative of aerosol inhomogeneity within the 80 km spatial domain used for AERONET comparison. In order to ensure that CALIPSO and AERONET observations refer to the same atmospheric volume, we constrain our dataset to horizontally homogeneous cases only, by removing

ACPD
13, 14749–14795, 2013

the cases with CALIPSO 5 km AOD relative variability over 10 %. Using this threshold, the averaged CALIPSO AODs for each overpass within a radius of 80 km from the AERONET stations are compared with AERONET AODs in the lower panel of Fig. 2. The comparison of the original CALIPSO product (LR = 40 sr) is shown to the left, while the same comparison but for LR = 58 sr is shown to the right. A Pearson's correlation coefficient of 0.92 reveals excellent agreement for both co-located datasets. Moreover, the use of the LR value of 58 sr improves the slope of the linear regression from 0.7 (for the original CALIPSO product) to 0.96 (for LR = 58 sr). Absolute biases between CALIPSO and AERONET AODs are down to −0.03 from −0.10, while the confidence parameters (t test scores and p values) show that the bias for the AODs computed with LR equal to 58 sr change from being statistically significant (with very high confidence for the original CALIPSO product) to non-significant (see also Table 1). We have to emphasize once again that the improvements refer only to the domain examined, i.e., the Sahara desert and Europe. Similar processing has also been performed for the Middle East (not shown here) and showed that the original CALIPSO product was in a very good agreement with AERONET. Thus an average LR of 40 sr applies well for that region, as already reported by Schuster et al. (2012).

3.2 CALIPSO comparison with MODIS

3.2.1 Comparison methodology

In this section, we compare 1° × 1° spatial averages of CALIPSO dust AODs with the co-located MODIS-Aqua Level 3 AOD product. Concerning CALIPSO, we use only cases for which the 5 km product is cloud free and the aerosol classification scheme reveals only dust presence in all profiles included in the 1° × 1° Aqua-MODIS cell. The CALIPSO data are screened by CAD score (−20 to −100), extinction QC flag (only aerosol layers with values 0, 1, 18 and 16) and extinction uncertainty (only data with reliable extinction retrievals having an uncertainty in the layers above them of less than 99.9 km^{-1}). Then, the average extinction profile for the 1° × 1° cell is calculated

ACPD
13, 14749–14795, 2013

Optimizing Saharan dust CALIPSO retrievals

V. Amiridis et al.

taking into account dust extinction values as well as zero extinction values for heights containing only molecules. The dust AOD used for the comparison is finally calculated by integrating the 5 km single extinction profiles and by averaging the final AODs within the cell.

The MODIS Level 3 product is also screened. We use AOD retrievals for which the MODIS-retrieved cloudiness is less than 20 % within the cell, in order to constrain our dataset to accurate, almost cloud-free retrievals. The criterion for cloudiness is rather strict if we consider that realistic aerosol MODIS products have been used in the literature for cloudiness levels less than 80 % (e.g., Zhang et al., 2005; Remer et al., 2008). However, our main concern for this comparison is to avoid a possible overestimation of MODIS AODs due to the presence of clouds, since it is well documented that clouds can lead to a significant overestimation of MODIS AOD, especially for cloud fractions higher than 80 % (e.g., Zhang et al., 2005; Remer et al., 2008). In addition to the cloudiness criterion, the MODIS Level 3 product is filtered in order to ensure the representativeness of the selected AOD values for the $1^{\circ} \times 1^{\circ}$ cell. To ensure this, we have selected Level 3 data produced from at least 60 Level 2 records of 10 km spatial resolution out of a maximum of 121 pixel counts, as input for the Level 3 aerosol data. It should be noted that, after filtering the dataset, 80 % of the selected cells are over maritime areas. This also increases the accuracy of MODIS AODs used, since over land the sensor is less reliable due to the fact that the retrievals are affected by higher surface reflectances (e.g., Remer et al., 2005, 2008).

The aforementioned constraints led to a significant decrease in size of the initial dataset, but maintained the "quality" of the selected cases. Spectral conversions are not applied and the final comparison is between AODs at 532 nm for CALIPSO AODs and 550 nm for MODIS.

3.2.2 Results and discussion

The final dataset of CALIPSO versus MODIS AOD consists of 178 cases for the 5 yr dataset and this comparison is presented in Fig. 3 for the original CALIPSO retrievals using the LR of 40 sr (left) and for the corrected product using the LR of 58 sr (right). The upper panel of Fig. 3 presents the dataset without constraints, while the lower panel shows the final 178 cells of our comparison based on applying the filters described in Sect. 3.2.1. The LR correction reveals an agreement with cloud-free MODIS AODs similar to that obtained from the AERONET comparison. The statistics of the comparison (presented in Table 2) shows an improved, statistically non-significant absolute bias for the corrected CALIPSO AOD equal to −0.02, much lower than the statistically significant bias for the original product of the order of −0.07. The slope of the linear regression between the two datasets improves from 0.73 to close to unity (0.97) and has a Pearson correlation coefficient for both comparisons of the order of 0.74. In conclusion, the two sensors show fairly good agreement for dust observations after the correction of the LR used in the CALIPSO algorithm when only cloud-free MODIS cells (less than 20 %) are acknowledged. Residuals in this comparison are most likely attributed to other retrieval errors for both sensors.

The agreement found between the two sensors in the case of dust shows that the dust LR issue is critical and should be taken into account in similar future work. Many studies in the literature have reported negative biases for CALIPSO AODs with respect to MODIS co-located Level 2 or Level 3 retrievals. For example, Kittaka et al. (2011) compared the CALIPSO Version 2 AOD at 532 nm with the MODIS-Aqua Level 2 AOD at 550 nm from June 2006 to August 2008. They found that the AOD from CALIPSO has a small global mean bias relative to MODIS. For Europe and the Mediterranean, CALIOP under-estimates MODIS by up to 0.1 (Fig. 9 of Kittaka et al., 2011). Redemann et al. (2012) assessed the consistency between instantaneously co-located Level 2 AODs from MODIS and CALIPSO Version 2 and 3 and found that the CALIPSO Version 3 product is generally in better agreement with MODIS AOD but shows however regional and seasonal variability in the absolute biases of the two sensors. For example, Fig. 8 in Redemann et al. (2012) shows a clear CALIPSO under-estimation of the order of 0.1 over Europe and the Mediterranean mostly during the spring and summer months, which are the seasons containing frequent Saharan dust advections.

ACPD
13, 14749–14795, 2013

Recently, Ma et al. (2012) compared Level 3 CALIPSO and Version 3 MODIS products in the context of four regions having large systematic biases. Their comparison showed that CALIPSO AOD is significantly lower than MODIS AOD over regions with dust influence during the whole time period, and that the maximum bias equaled −0.3 over the Sahara region. Winker et al. (2013) concurred with the aforementioned low CALIPSO biases, but added that MODIS AOD accuracy decreases as the environment becomes cloudier (e.g. Zhang and Reid, 2006). The methodology and results presented in this section suggest that constraints regarding the dust LR, cloudiness and the representativeness of cell samples have to be applied to both sensors in order for them to be comparable.

3.3 CALIPSO comparison with BSC-DREAM8b simulated dust fields

The CALIPSO evaluation study against AERONET and MODIS observations in Sects. 3.1 and 3.2 respectively, points to the need for a larger average LR (of the order of 58 sr) for the dust component of the CALIPSO retrieval algorithm over the domain examined in our work. This correction is expected to eliminate the negative bias of CALIPSO AODs reported in the literature, especially over the Saharan desert and surrounding regions. In order to evaluate the impact of a larger LR on climatological averages, specifically the recently released Level 3 CALIPSO climatological product, we evaluate in this section this product against dust simulations from the BSC-DREAM8b regional dust model. In addition to the original Level 3 CALIPSO product and the amended product using a LR equal to 58 sr, a third product is evaluated that uses both a corrected value of LR equal to 58 sr as well as corrections that account for the pure dust component included in dust and polluted dust CALIPSO subtypes.

3.3.1 Comparison methodology

In this section we present the methodology followed for the comparison and the production of the three versions of climatological products used in our study:

ACPD
13, 14749–14795, 2013

- *Version I:* the original CALIPSO Level 3 dust extinction product with LR equal to 40 sr, based on the original CALIPSO averaging scheme,
- *Version II:* a dust extinction product retrieved by the application of an LR equal to 58 sr on Level 2 backscatter profiles based on the original CALIPSO averaging scheme, and
- *Version III:* a product retrieved by the application of LR equal to 58 sr together with an averaging scheme different to CALIPSO that: (1) acknowledges zero extinction values for non-dust aerosol types detected in the cell, and (2) corrects for pure dust by separating the pure dust component from the dust and polluted dust subtypes.

The three versions are compared with co-located and synchronized dust extinction simulations from the BSC-DREAM8b model. Vertical averaging is applied to the CALIPSO products in order to vertically co-locate extinction values with the model's vertical resolution. No spectral correction is applied since dust particles are expected to have a weak spectral dependence on extinction (e.g. O'Neill et al., 2003; Schuster et al., 2006). As a result, the CALIPSO extinction at 532 nm is directly compared with the BSC-DREAM8b extinction at 550 nm. Our comparison is applied to data spanning the period January 2007 to December 2010. The methodology followed for the production of the different versions of CALIPSO climatological dust products is described below.

Version I: the methodology followed for the production of the original CALIPSO $1^{\circ} \times 1^{\circ}$ monthly mean dust extinction product is based on the averaging and screening techniques introduced by the CALIPSO team for the Level 3 climatology (Winker et al., 2013, and Appendix therein). CALIOP Version 3 aerosol extinction profiles at 532 nm are aggregated onto $1^{\circ} \times 1^{\circ}$ grids and monthly mean extinction profiles are computed for aerosol species classified as dust. Following the definitions of the CALIPSO Level 3 climatology, we use the cloud-free product only. In brief, the CALIPSO Level 2

Discussion Paper | Discussion Paper | Discussion Paper | Discussion Paper |
ACPD
13, 14749–14795, 2013
Optimizing Saharan dust CALIPSO retrievals
V. Amiridis et al.

data are screened by CAD score (use only data with CAD score between −20 and −100), extinction QC flag (only aerosol layers with values 0, 1, 18 and 16 are accepted), and extinction uncertainty (use only data with reliable extinction retrievals having uncertainty in the layers above them, less than 99.9 km^{-1}). Additional filters are applied in order to screen misclassified clouds, isolated layers due to noise spikes, sub-surface samples, samples below opaque cloud and aerosol layers, large negative near-surface extinction samples, surface contamination beneath surface-attached opaque layers, and undetected surfaces associated with low aerosol biases. In clear air, the extinction value is set to zero (for details, see Winker et al., 2013, and https://eosweb.larc.nasa.gov/sites/default/files/project/calipso/quality_summaries/CALIOP_L3AProProducts_1-00.pdf). In order to validate the ability of our Version 1 product to reproduce the CALIPSO Level 3 averaging scheme, the algorithm developed in this study has been evaluated against the original CALIPSO product that is distributed on a $5^{\circ} \times 2^{\circ}$ longitude–latitude spatial resolution grid. The comparison revealed that the Level 3 retrievals obtained from both algorithms are in excellent agreement, having a Pearson correlation coefficient of 0.98 and a linear regression slope of approximately 1.0 in the case of a test comparison of global extinction retrievals for January 2008 (not shown here). After validating the algorithm, the method was applied to $1^{\circ} \times 1^{\circ}$ spatial resolution aggregations of Level 2 products for the domain of interest, so that the monthly averaged products could be compared with the results of BSC-DREAM8b dust simulations.

We should note here, that for the comparison of the CALIPSO Level 3 dust product with BSC-DREAM8b, we used both day-time and night-time CALIPSO products. The original Level 3 CALIPSO product distinguishes between day-time and night-time profiles, since for the day-time product the solar background reduces the aerosol detection sensitivity and results in smaller column AODs (Winker et al., 2013). Differences between day-time and night-time products can be attributed to tuning of the retrieval algorithms to account for differences in signal to noise ratios (Winker et al., 2013). However, differences between the day-time and night-time Level 3

ACPD
13, 14749–14795, 2013

product could be also attributed to sampling differences since, due to its orbit pattern, CALIPSO samples different geographical areas during day and night orbits. Moreover, aerosol loads can have large diurnal variations depending on the region and result in real, rather than artificial differences between the day-time and night-time product. For the domain of our study we do not distinguish between lightning conditions, following the small reported differences between the day-time and night-time product reported in Winker et al. (2013) for zonally-averaged mean aerosol extinction during the summer months between 2006 and 2011 (Fig. 7 of Winker et al., 2013). These findings suggest that the ratio between the day-time and night-time climatological extinction product is close to unity for the latitude zone between 20 and 50 degrees that includes the Saharan desert, the Mediterranean and a large part of Europe.

Version II: this version follows the definitions of the CALIPSO Level 3 product (Version I) with regard to the data averaging and screening procedures. The only alteration applied regards the production of extinction profiles from the dust backscatter profiles which are multiplied by the LR of 58 sr.

Version III: in this version, the LR used for the production of extinction profiles is kept equal to 58 sr as in Version II. However, two alterations are introduced; the first regards the vertically-resolved separation of pure dust from aerosol types reported as dust and polluted dust, and the second involves the CALIPSO averaging scheme.

Regarding the first alteration, the separation of the pure dust component is obtained by applying the method introduced by Tesche et al. (2009a). This method makes use of the particle backscatter coefficient and the particle depolarization ratio at 532 nm in order to separate the backscatter contributions of the weakly light-depolarizing aerosol components ("other type") from the contribution of strongly light-depolarizing particles (pure dust). In order to define the dust mixtures in our study, we first examined CALIPSO conventions regarding its classification scheme. In general, dust presence in the atmosphere is classified by CALIPSO either as "Dust", meaning pure dust, or

"Polluted Dust", meaning dust mixed with other non-depolarizing aerosols. These types are distinguished by the CALIPSO algorithm using the only available Level 1 intensive aerosol property capable of classifying non-spherical particles, namely the volume depolarization (Omar et al., 2009). From the volume depolarization, an approximate particle depolarization ratio is calculated by:

$$\delta_{p}^{est} = \frac{\delta_{v}[(R-1)(1+\delta_{m})+1]-\delta_{m}}{(R-1)(1+\delta_{m})+\delta_{m}-\delta_{v}} \quad (3)$$

where δ_v indicates the volume depolarization, δ_m is the molecular depolarization, and R is the total scattering ratio, equal to the ratio of the total backscatter to the molecular backscatter. The approximate aerosol depolarization ratio is affected by the total scattering ratio which is not corrected for attenuation of the laser beam between the satellite and the layer under investigation. This leads to over-estimation of the actual particle depolarization ratio and correspondingly affects the classification of dust into pure dust or polluted dust. Recent CALIPSO validation results using airborne High Spectral Resolution Lidar (HSRL) co-located measurements (Burton et al., 2013), show that the CALIPSO dust classification corresponds to a classification of either dust or dust mixtures by HSRL. This is attributed by the authors to either the over-estimation of the approximated aerosol depolarization or to the polarization thresholds used by the CALIPSO classification algorithm. To be specific, while the threshold for the approximate particle depolarization regarding the pure dust classification of CALIPSO is 0.2, the particle depolarization ratios for pure dust reported in the literature is much higher. Particle depolarization ratios measured over the Sahara during the SAMUM-1 campaign, were found to be of the order of 0.31 ± 0.03 at 532 nm (e.g. Freudenthaler et al., 2009). Values of 0.35 have also been reported in the literature for Asian dust from long-term observations over China and Japan (Sugimoto et al., 2003; Shimizu et al., 2004). Thus, Burton et al. (2013) finding that pure dust CALIPSO classifications can, in reality, be dust mixtures (according to HSRL) is not surprising.

In Version III of our climatological product, we treat both dust and polluted dust types as dust mixtures and assume a value of 0.33 for the particle depolarization ratio of pure

ACPD
13, 14749–14795, 2013

dust, as confirmed by ground measurements (e.g. Freudenthaler et al., 2009). In order to examine the true particle depolarization of the layers included in our study instead of relying on the Level 1 approximated value used for the classification, we calculated the reported CALIPSO Level 2 particle depolarization ratio for each layer and present their distribution in Fig. 4 (black line). In the same Figure, a second distribution is also presented (red line), representing the particle depolarization ratios retrieved for the same dataset using the standard equation:

$$\delta_p = \frac{\beta_{perp}}{\beta_t - \beta_{perp}} \tag{4}$$

where β_t is the CALIPSO Level 2 total backscatter and β_{perp} is the perpendicular backscatter product. The results for the standard depolarization formula (Eq. 4) have been found to be different from those using the particle depolarization ratio product reported by CALIPSO Level 2. This finding has been already reported by Tesche et al. (2013). The authors state that this inconsistency is currently under investigation by the CALIPSO team and is most likely attributed to a software error in the CALIPSO retrieval algorithm. The differences for our dataset are presented in Fig. 4. In the upper panel of Fig. 4, the distribution of particle depolarization ratios is presented for the layers characterized as polluted dust, while the lower panel refers to layers classified as dust by the CALIPSO scheme using the Level 1 product's approximation of the particle depolarization ratio (Omar et al., 2009). The gray-shaded areas denote the approximate depolarization ranges for the classification of polluted dust (0.075 < depolarization < 0.2) and pure dust (depolarization > 0.2). The corrected distributions for pure dust (Fig. 4 – lower panel) show values lower than 0.5, ranging mainly between 0.15 and 0.4. Most of the values are greater than the threshold value of 0.2 for the Level 1 approximate depolarization product, suggesting that the classification is mostly justified by the Level 2 particle depolarization as well. The maximum of the distribution is found at 0.3, which is in good agreement with ground-truth particle depolarization values measured over Sahara during the SAMUM-1 campaign (e.g.

ACPD
13, 14749–14795, 2013

Freudenthaler et al., 2009). The distribution of the original CALIPSO particle depolarization is skewed towards higher values, which are often unrealistic. Regarding the distribution for the polluted dust type (upper panel), this is again within the range of values intended to be used as thresholds for classification purposes based on Level 1 approximations. This is true especially for the corrected values produced by Eq. (4) (red), which in general are shifted to lower values.

All the above considerations are consolidated in the methodology followed for producing the Version III climatological product. We separate the pure dust component included in dust mixtures (either classified as dust or polluted dust) by using the methodology of Tesche et al. (2009a) and apply the correct particle depolarization ratios using Eq. (4). Because the 5 km Level 2 CALIPSO depolarization profile is mostly noisy, we chose also to use a layer-averaged depolarization value for our corrections. This is done by applying Eq. (4) to layer-averaged perpendicular and total backscatter values. The corrected particle depolarization ratios are then used to apply the method of Tesche et al. (2009a). As already mentioned, the method makes use of the particle backscatter coefficient and the particle depolarization ratio at 532 nm in order to separate the backscatter contributions of the weakly light-depolarizing aerosol components from the contribution of strongly light-depolarizing particles. To be more specific, the method assumes that if we have two aerosol types, the backscatter contribution of the first aerosol type β_1, is obtained from the measured total backscatter coefficient β_t by:

$$\beta_1 = \beta_t \frac{(\delta_p - \delta_2)(1 + \delta_1)}{(\delta_1 - \delta_2)(1 + \delta_p)} \tag{5}$$

where δ_p is the observed particle depolarization ratio and δ_2, δ_1 are the assumed "typical" particle depolarization ratios of the two pure aerosol types. The particle backscatter coefficient of the second aerosol type is given by $\beta_t - \beta_1$. In our interpretation of the method, we assume as mixtures all CALIPSO dust types (dust and polluted dust), acknowledging as pure dust only those layers having depolarization values greater than 0.33 (e.g. Freudenthaler et al., 2009). A value of 0.33 was used for the linear parti-

ACPD
13, 14749–14795, 2013

cle depolarization of pure dust in Eq. (5) (aerosol type 1) while a value of 0.03 was considered for the non-depolarizing aerosol type 2 in our separation procedure. This methodology is demonstrated in the example of Fig. 5. For the selected profile, the classification of CALIPSO revealed a dust layer between 0 and 1.5 km and an elevated polluted dust layer between 1.5 and 3.2 km (Fig. 5 – left panel). The level 2 layer-mean particle depolarization ratio (Fig. 5 – middle panel), shows values of the order of 0.3 for the dust layer (green) and 0.25 for the polluted dust layer. The red lines represent the corrected layer-averaged particle depolarization ratios derived by the application of Eq. (4). Using the corrected depolarization values and applying the method of Tesche et al. (2009a) on the backscatter Level 2 CALIPSO product (Eq. 5), we finally retrieve the result presented in the right panel of Fig. 5, where the pure dust backscatter has been separated from the "other" aerosol type of particle depolarization ratio equal to 0.03 (assumed to be present in the dust mixture). The pure dust backscatter profile is then multiplied by the the LR of 58 sr in order to retrieve the pure dust extinction coefficient.

After producing the pure dust extinctions for Version III, we aggregate the profiles on a $1^{\circ} \times 1^{\circ}$ cell. The averaging procedure for dust is altered from the original CALIPSO methodology followed for Version I and II, by introducing in the averaging scheme non-dust observations beyond those of clear air, namely the presence of other aerosol types detected by CALIPSO (Marine, Clean Continental, Polluted Continental, Smoke). These types are taken into consideration in the Version III averaging routine as zero extinction values and not as "non-available" observations as is the case in the CALIPSO Level 3 algorithm (Version I and II). To demonstrate how this averaging scheme performs in contrast to the CALIPSO methodology, an example of our approach is given in Fig. 6. One $1^{\circ} \times 1^{\circ}$ degree scene is presented where the aerosol classification scheme shows the presence of dust, polluted dust and marine aerosol subtypes. Version I, II and III extinction averages are presented in the right panel of Fig. 6. Version II shows larger extinction values due to the use of a larger LR (58 sr). The acknowledgment of dust mixtures and respective dust contributions in Version III causes significant differences from the other versions. In particular, it leads to lower values of dust extinction in general, but especially between the surface and 0.5 km since, in this height range, we acknowledge as zero values the extinction values corresponding to the marine subtype. Moreover, Version III retrieves dust extinction by separating pure dust from polluted dust in the height range between 1.5 and 2.7 km. Contrast with this, Versions I and II retrieve for the same height range zero extinction, since only the polluted dust type is present (which is not acknowledged).

3.3.2 Results and discussion

The comparison of monthly mean AODs for the domain of our study obtained from all the three versions of $1^{\circ} \times 1^{\circ}$ Level 3 products is presented in Fig. 7. All AODs refer to integrals of the extinction profiles in the vertical range between the maximum surface elevation of the cell and a height of 8 km. The colour bar represents the latitudinal zone of the comparison, in 5 degree bins. While Pearson's correlation coefficient remains almost constant for all Versions around 0.87, we observe a significant improvement in the regression slopes for Version II and Version III which increase to 0.73 from 0.5 with reference to the CALIPSO original Version I. A significant improvement is also visible in the absolute biases for Version II and III which reduce to the value −0.01 compared with −0.05 for Version I. As expected, the AOD shows a latitudinal dependence having larger values over Africa and lower values over Northern Europe.

In Fig. 8 we present the vertically-resolved comparisons averaged over the domain of our study. The upper left panel shows the mean extinction profiles resulting from BSC-DREAM8b simulations and for all three CALIPSO climatological Versions I–III examined. While the original CALIPSO Version I mostly under-estimates model simulations, Version II seems to over-estimate them. Furthermore, the use of a dust LR equal to 58 sr to correct for the global mean value of 40 sr in Version II, does not seem to give satisfactory results in relation to the BSC-DREAM8b model, contrary to the results of our comparison with AERONET and MODIS. However, this is most likely attributable to the averaging procedure and the mixing of dust with other types, since we obtain a very satisfactory agreement with Version III where the same LR of 58 sr has been used as well. The agreement of Version III with the model is clearly visible for the lower troposphere where most of the mixing of dust with aerosol types from ground or sea sources is expected to occur. The absolute biases presented in the upper-right panel of Fig. 8 point to the same conclusions. In the same plot, the vertically-averaged absolute biases are presented as well. The black line represents the reported model bias over the domain, as this is retrieved from comparison with AERONET observations (Basart et al., 2012). The results of Version I and III are close to this bias, showing that the best agreement with the model is achieved for these two versions. However, when linearly regressing Version I and III on the BSC-DREAM8b model as a function of height, the Pearson correlation coefficients show better agreement for Version III, especially for height ranges between the ground and 4 km (lower-left panel of Fig. 8). The regression slopes also show better agreement for Version III, reaching values closest to unity (lower-right panel of Fig. 8).

The spatial distribution of 5 yr AOD absolute biases when comparing the model and the three versions examined is presented in Fig. 9. The columnar biases show a significant improvement over Northern Africa for Versions II and III. For the Sahel region however, Versions II and III over-estimate when compared to the model. However, the biases observed over the Sahel and North-Western Africa fall within regions of model under-estimation and over-estimation respectively. This is reported in the detailed evaluation of BSC-DREAM8b against AERONET published by Basart et al. (2012). The results of this study are geographically summarized in Fig. 10 where the radii of the circles correspond to the model biases with respect to AERONET. Biases lower than 0.1 were found over Western, Central and Eastern regions in the Mediterranean, and a bias close to 0.1 is reported for the Atlantic region. The model evaluation results as compared with AERONET, have a better spatial agreement with the comparison made with the CALIPSO Version III climatological product, as shown in Fig. 9 (lower panel). Version II clearly over-estimates over Europe (especially Eastern Europe), the Mediterranean and especially the Atlantic. Version I on the other hand, under-estimates the BSC-DREAM8b model in almost the whole domain, and especially over source regions in Northern Africa. If we compare Versions II and III, taking into account known model biases (Fig. 10), then we can conclude that the LR correction improves biases over Northern Africa, while the correction in Version III for pure dust retrievals from dust mixtures improves significantly over Europe, where more mixing is expected.

4 Summary and conclusions

CALIPSO is capable of providing a multi-year, robust 4-D dust climatology, a task that cannot easily be achieved by passive sensors, especially over deserts. However, limitations on retrieval performance using CALIPSO exist, especially regarding the classification of dust and its mixtures based on the approximate particle depolarization and the LR assumption. In this paper we show the potential improvement of CALIPSO dust retrievals over Europe and North Africa by using a dust LR of 58 sr, demonstrating that a regional correction is feasible when using a universal and spatially constant LR. Moreover, improvements in the Level 3 climatological product for dust are demonstrated when comparing with BSC-DREAM8b dust simulations. This is achieved by altering the CALIPSO Level 3 averaging scheme so as to account for the pure dust component in dust mixtures and to acknowledge the presence of other, non-dust aerosol types rather than only dust and clear air. Combining the calculations with the LR-correction for the region examined, the results are in better agreement with the dust model simulations.

The agreement presented here will facilitate and hopefully encourage accurate, climatological dust studies in this large geographical domain. Future work could include the application of the methodology in similar studies over the deserts in the Middle East and China in order to optimize CALIPSO dust retrievals over these areas as well. Ground-based measurements of the dust LR for these regions will be vital for the success of implementing similar improvements.

Accurate climatological CALIPSO extinction retrievals could also help form a bridge between CALIPSO time series and future ESA ADM-Aeolus and EarthCARE retrievals, in order to accomplish a multi-decadal climatological record. Such efforts are considered feasible especially for dust, since this aerosol type has a relatively small wavelength dependence and it should be straight-forward to combine CALIPSO products in the visible with future EarthCARE products in the ultraviolet spectral region.

Finally, the agreement between CALIPSO and MODIS reported in this study is encouraging for future combinations of paired data from the two sensors. Such synergy will help the community make further deductions about aerosol types and origin, and facilitate at the same time the evaluation of for example the Deep Blue product over the Sahara and potentially other deserts.

Acknowledgements. This work has been developed under the auspices of the ESA-ESTEC project: Lidar Climatology of Vertical Aerosol Structure for Space-Based LIDAR Simulation Studies (LIVAS) contract No. 4000104106/11/NL/FF/fk. CALIPSO data were obtained from the NASA Langley Research Center Atmospheric Science Data Center. The research leading to these results has received funding from the European Union Seventh Framework Programme (FP7/2007-2013) under grant agreement no 262254 (ACTRIS). S.K. would like to acknowledge ACI-UV (FP7-PEOPLE-2009-RG Marie Curie European Reintegration Grant, PERG05-GA-2009-247492). MT is supported by the Marie-Curie IEF funded project "AEROMAP: Global mapping of aerosol properties using neural network inversions of ground and satellite based data", grant agreement No. 300515.

References

Amiridis, V., Kafatos, M., Perez, C., Kazadzis, S., Gerasopoulos, E., Mamouri, R. E., Papayannis, A., Kokkalis, P., Giannakaki, E., Basart, S., Daglis, I., and Zerefos, C.: The potential of the synergistic use of passive and active remote sensing measurements for the validation of a regional dust model, Ann. Geophys., 27, 3155–3164, doi:10.5194/angeo-27-3155-2009, 2009.

Balis, D. S., Amiridis, V., Nickovic, S., Papayannis, A., and Zerefos, C.: Optical properties of Saharan dust layers as detected by a Raman lidar at Thessaloniki, Greece, Geophys. Res. Lett., 31, L13104, doi:10.1029/2004GL019881, 2004.

Barnaba, F. and Gobbi, G. P.: Aerosol seasonal variability over the Mediterranean region and relative impact of maritime, continental and Saharan dust particles over the basin from MODIS data in the year 2001, Atmos. Chem. Phys., 4, 2367–2391, doi:10.5194/acp-4-2367-2004, 2004.

Basart, S., Pérez, C., Nickovic, S., Cuevas, E., and Baldasano, J.: Development and evaluation of the BSC-DREAM8b dust regional model over northern Africa, the Mediterranean and the Middle East, Tellus B, 64, 18539, doi:10.3402/tellusb.v64i0.18539, 2012.

Burton, S. P., Ferrare, R. A., Vaughan, M. A., Omar, A. H., Rogers, R. R., Hostetler, C. A., and Hair, J. W.: Aerosol classification from airborne HSRL and comparisons with the CALIPSO vertical feature mask, Atmos. Meas. Tech. Discuss., 6, 1815–1858, doi:10.5194/amtd-6-1815-2013, 2013.

D'Almeida, G. A.: On the variability of desert aerosol radiative characteristics, J. Geophys. Res., 92, 3017–3026, 1987.

Freudenthaler, V., Esselborn, M., Wiegner, M., Heese, B., Tesche, M., Ansmann, A., Muller, D., Althausen, D., Wirth, M., Fix, A., Ehret, G., Knippertz, P., Toledano, C., Gasteiger, J., Garhammer, M., and Seefeldner, M.: Depolarization ratio profiling at several wavelengths in pure Saharan dust during SAMUM 2006, Tellus B, 61, 165–179, doi:10.1111/j.1600-0889.2008.00396.x, 2009.

Haustein, K., Pérez, C., Baldasano, J. M., Müller, D., Tesche, M., Schladitz, A., Esselborn, M., Weinzierl, B., Kandler, K., and Von Hoyningen-Huene, W.: Regional dust model performance during SAMUM 2006, Geophys. Res. Lett., 36, L03812, doi:10.1029/2008GL036463, 2009.

Holben, B. N., Tanré, D., Smirnov, A., Eck, T. F., Slutsker, I., Abuhassan, N., Newcomb, W. W., Schafer, J. S., Chatenet, B., Lavenu, F., Kaufman, Y. J., Vande Castle, J., Setzer, A., Markham, B., Clark, D., Frouin, R., Halthore, R., Karneli, A., O'Neill, N. T., Pietras, C., Pinker, R. T., Voss, K., and Zibordi, G.: An emerging ground-based aerosol climatology: aerosol optical depth from AERONET, J. Geophys. Res.-Atmos., 106, 12067–12097, doi:10.1029/2001JD900014, 2001.

Hsu, N. C., Tsay, S. C., King, M. D., and Herman, J. R.: Aerosol properties over bright-reflecting source regions, IEEE T. Geosci. Remote, 42, 557–569, 2004.

ACPD
13, 14749–14795, 2013

Optimizing Saharan dust CALIPSO retrievals

V. Amiridis et al.

Ichoku, C., Chu, D. A., Mattoo, S., Kaufman, Y. J., Remer, L. A., Tanré, D., Slutsker, I., and Holben, B. N.: A spatio-temporal approach for global validation and analysis of MODIS aerosol products, Geophys. Res. Lett., 29, 8006, doi:10.1029/2001GL013206, 2002.
Janjic, Z. I.: The Step-Mountain Eta Coordinate Model: further developments of the convection, viscous sublayer and turbulence closure schemes, Mon. Weather Rev., 122, 927–945, 1994.
Kittaka, C., Winker, D. M., Vaughan, M. A., Omar, A., and Remer, L. A.: Intercomparison of column aerosol optical depths from CALIPSO and MODIS-Aqua, Atmos. Meas. Tech., 4, 131–141, doi:10.5194/amt-4-131-2011, 2011.
Kacenelenbogen, M., Vaughan, M. A., Redemann, J., Hoff, R. M., Rogers, R. R., Ferrare, R. A., Russell, P. B., Hostetler, C. A., Hair, J. W., and Holben, B. N.: An accuracy assessment of the CALIOP/CALIPSO version 2/version 3 daytime aerosol extinction product based on a detailed multi-sensor, multi-platform case study, Atmos. Chem. Phys., 11, 3981–4000, doi:10.5194/acp-11-3981-2011, 2011.
Kokkalis, P., Mamouri, R. E., Todua, M., Didebulidze, G. G., Papayannis, A., Amiridis, V., Basart, S., Pérez, C., and Baldasano, J. M.: Ground-, satellite- and simulation-based analysis of a strong dust event over Abastumani, Georgia, during May 2009, Int. J. Remote Sens., 33, 4886–4901, doi:10.1080/01431161.2011.644593, 2012.
Levy, R. C., Remer, L. A., Kleidman, R. G., Mattoo, S., Ichoku, C., Kahn, R., and Eck, T. F.: Global evaluation of the Collection 5 MODIS dark-target aerosol products over land, Atmos. Chem. Phys., 10, 10399–10420, doi:10.5194/acp-10-10399-2010, 2010.
Liu, Z., Omar, A., Vaughan, M., Hair, J., Kittaka, C., Hu, Y., Powell, K., Trepte, C., Winker, D., Hostetler, C., Ferrare, R., and Pierce, R.: CALIPSO lidar observations of the optical properties of Saharan dust: a case study of long-range transport, J. Geophys. Res., 113, D07207, doi:10.1029/2007JD008878, 2008.
Liu, Z., Vaughan, M., Winker, D., Kittaka, C., Getzewich, B., Kuehn, R., Omar, A., Powell, K., Trepte, C., and Hostetler, C.: The CALIPSO Lidar Cloud and Aerosol Discrimination: version 2 algorithm and initial assessment of performance, J. Atmos. Ocean. Tech., 26, 1198–1213, doi:10.1175/2009jtecha1229.1, 2009.
Loeb, N. G. and Manalo-Smith, N.: Top-of-atmosphere direct radiative effect of aerosols over global oceans from merged CERES and MODIS observations, J. Climate, 18, 3506–3526, doi:10.1175/JCLI3504.1, 2005.

ACPD
13, 14749–14795, 2013

Ma, X., Bartlett, K., Harmon, K., and Yu, F.: Comparison of AOD between CALIPSO and MODIS: significant differences over major dust and biomass burning regions, Atmos. Meas. Tech. Discuss., 5, 8343–8367, doi:10.5194/amtd-5-8343-2012, 2012.
Mattis, I., Ansmann, A., Müller, D., Wandinger, U., and Althausen, D.: Dual-wavelength Raman lidar observations of the extinction-to-backscatter ratio of Saharan dust, Geophys. Res. Lett., 29, 1306, doi:10.1029/2002GL014721, 2002.
Mattis, I., Müller, D., Ansmann, A., Wandinger, U., Preißler, J., Seifert, P., and Tesche, M.: Ten years of multiwavelength Raman lidar observations of free-tropospheric aerosol layers over central Europe: geometrical properties and annual cycle, J. Geophys. Res.-Atmos., 113, D20202, doi:10.1029/2007JD009636, 2008.
Mona, L., Amodeo, A., Pandolfi, M., and Pappalardo, G.: Saharan dust intrusions in the Mediterranean area: three years of Raman lidar measurements, J. Geophys. Res., 111, D16203, doi:10.1029/2005JD006569, 2006.
Nickovic, S., Kallos, G., Papadopoulos, A., and Kakaliagou, O.: Model for prediction of desert dust cycle in the atmosphere, J. Geophys. Res., 106, 18113–18129, 2001.
O'Neill, N. T., Eck, T. F., Smirnov, A., Holben, B. N., and Thulasiraman, S.: Spectral discrimination of coarse and fine mode optical depth, J. Geophys. Res., 108, 4559, doi:10.1029/2002JD002975, 2003.
Omar, A. H., Winker, D. M., Kittaka, C., Vaughan, M. A., Liu, Z. Y., Hu, Y. X., Trepte, C. R., Rogers, R. R., Ferrare, R. A., Lee, K. P., Kuehn, R. E., and Hostetler, C. A.: The CALIPSO automated aerosol classification and lidar ratio selection algorithm, J. Atmos. Ocean. Tech., 26, 1994–2014, doi:10.1175/2009jtecha1231.1, 2009.
Papayannis, A., Amiridis, V., Mona, L., Tsaknakis, G., Balis, D., Bösenberg, J., Chaikovski, A., De Tomasi, F., Grigorov, I., Mattis, I., Mitev, V., Müller, D., Nickovic, S., Pérez, C., Pietruczuk, A., Pisani, G., Ravetta, F., Rizi, V., Sicard, M., Trickl, T., Wiegner, M., Gerding, M., Mamouri, R. E., D'Amico, G., and Pappalardo, G.: Systematic lidar observations of Saharan dust over Europe in the frame of EARLINET (2000–2002), J. Geophys. Res.-Atmos., 113, D10204, doi:10.1029/2007JD009028, 2008.
Pappalardo, G., Wandinger, U., Mona, L., Hiebsch, A., Mattis, I., Amodeo, A., Ansmann, A., Seifert, P., Linné, H., Apituley, A., Arboledas, L. A., Balis, D., Chaikovsky, A., D'Amico, G., De Tomasi, F., Freudenthaler, V., Giannakaki, E., Giunta, A.,Grigorov, I., Iarlori, M., Madonna, F., Mamouri, R.E., Nasti, L., Papayannis, A., Pietruczuk, A., Pujadas, M., Rizi, V., Rocadenbosch, F., Russo, F., Schnell, F., Spinelli, N., Wang, X., and Wiegner, M.: EARLINET cor-

relative measurements for CALIPSO: first intercomparison results, J. Geophys. Res., 115, D00H19, doi:10.1029/2009JD012147, 2010.

Pay, M. T., Piot, M., Jorba, O., Gassó, S., Gonçalves, M., Basart, S., Dabdub, D., Jiménez-Guerrero, P., and Baldasano, J. M.: A full year evaluation of the CALIOPE-EU air quality modeling system over Europe for 2004, Atmos. Environ., 44, 3322–3342, doi:10.1016/j.atmosenv.2010.05.040, 2010.

Pérez, C., Nickovic, S., Baldasano, J. M., Sicard, M., Rocadenbosch, F., and Cachorro, V. E.: A long Saharan dust event over the western Mediterranean: lidar, sun photometer observations, and regional dust modeling, J. Geophys. Res.-Atmos., 111, D15214, doi:10.1029/2005JD006579, 2006a.

Pérez, C., Nickovic, S., Pejanovic, G., Baldasano, J. M., and Özsoy, E.: Interactive dust-radiation modeling: a step to improve weather forecasts, J. Geophys. Res.-Atmos., 111, D16206, doi:10.1029/2005JD006717, 2006b.

Redemann, J., Vaughan, M. A., Zhang, Q., Shinozuka, Y., Russell, P. B., Livingston, J. M., Kacenelenbogen, M., and Remer, L. A.: The comparison of MODIS-Aqua (C5) and CALIOP (V2 & V3) aerosol optical depth, Atmos. Chem. Phys., 12, 3025–3043, doi:10.5194/acp-12-3025-2012, 2012.

Remer, L. A., Tanré, D., Kaufman, Y. J., Ichoku, C., Mattoo, S., Levy, R., Chu, D. A., Holben, B., Dubovik, O., Smirnov, A., Martins, J. V., Li, R.-R., and Ahman, Z.: Validation of MODIS aerosol retrieval over ocean, Geophys. Res. Lett., 29, 8008, doi:10.1029/2001GL013204, 2002.

Remer, L. A., Kaufman, Y. J., Tanré, D., Mattoo, S., Chu, D. A., Martins, J. V., Li, R.-R., Ichoku, C., Levy, R. C., Kleidman, R. G., Eck, T. F., Vermote, E., and Holben, B. N.: The MODIS aerosol algorithm, products, and validation, J. Atmos. Sci., 62, 947–973, doi:10.1175/JAS3385.1, 2005.

Remer, L. A., Kleidman, R. G., Levy, R. C., Kaufman, Y. J., Tanré, D., Mattoo, S., Martins, J. V., Ichoku, C., Koren, I., Yu, H., and Holben, B. N.: Global aerosol climatology from the MODIS satellite sensors, J. Geophys. Res.-Atmos., 113, D14S07, doi:10.1029/2007JD009661, 2008.

Shimizu, A., Sugimoto, N., Matsui, I., Arao, K., Uno, I., Murayama, T., Kagawa, N., Aoki, K., Uchiyama, A., and Yamazaki, A.: Continuous observations of Asian dust and other aerosols by polarization lidar in China and Japan during ACE-Asia, J. Geophys. Res., 109, D19S17, doi:10.1029/2002JD003253, 2004.

Schuster, G., Dubovik, O., and Holben, B.: Angstrom exponent and bimodal aerosol size distributions, J. Geophys. Res., 111, D07207, doi:10.1029/2005JD006328, 2006.
Schuster, G. L., Vaughan, M., MacDonnell, D., Su, W., Winker, D., Dubovik, O., Lapyonok, T., and Trepte, C.: Comparison of CALIPSO aerosol optical depth retrievals to AERONET measurements, and a climatology for the lidar ratio of dust, Atmos. Chem. Phys., 12, 7431–7452, doi:10.5194/acp-12-7431-2012, 2012.
Shao, Y., Raupach, M. R., and Findlater, P. A.: Effect of saltation bombardment on the entrainment of dust by wind, J. Geophys. Res., 98, 12719–12726, 1993.
Sugimoto, N., Matsui, I., Shimizu, A., Uno, I., Asai, K., Endoh, T., and Nakajima, T.: Observation of dust and anthropogenic aerosol plumes in the Northwest Pacific with a two-wavelength polarization lidar on board the research vessel Mirai, Geophys. Res. Lett., 29, 1901, doi:10.1029/2002GL015112, 2002.
Tegen, I. and Lacis, A. A.: Modeling of particle size distribution and its influence on the radiative properties of mineral dust aerosol, J. Geophys. Res., 101, 19237–19244, 1996
Tesche, M., Ansmann, A., Müller, D., Althausen, D., Engelmann, R., Freudenthaler, V., and Groß, S.: Vertically resolved separation of dust and smoke over Cape Verde using multi-wavelength Raman and polarization lidars during Saharan Mineral Dust Experiment 2008, J. Geophys. Res.-Atmos., 114, D13202, doi:10.1029/2009JD011862, 2009a.
Tesche, M., Ansmann, A., Müller, D., Althausen, D., Mattis, I., Heese, B., Freudenthaler, V., Wiegner, M., Esselborn, M., Pisani, G., and Knippertz, P.: Vertical profiling of Saharan dust with Raman lidars and airborne HSRL in southern Morocco during SAMUM, Tellus B, 61, 144–164, doi:10.1111/j.1600-0889.2008.00390.x, 2009b.
Tesche, M., Wandinger, U., Ansmann, A., Althausen, D., Müller, D., and Omar, A. H.: Ground-based validation of CALIPSO observations of dust and smoke in the Cape Verde region, J. Geophys. Res., 118, 1–14, doi:10.1002/jgrd.50248, 2013.
Todd, M. C., Bou Karam, D., Cavazos, C., Bouet, C., Heinold, B., Baldasano, J. M., Cautenet, G., Koren, I., Perez, C., Solmon, F., Tegen, I., Tulet, P., Washington, R., and Zakey, A.: Quantifying uncertainty in estimates of mineral dust flux: an intercomparison of model performance over the Bodélé depression, northern Chad, J. Geophys. Res.-Atmos., 113, D24107, doi:10.1029/2008JD010476, 2008.
Vaughan, M. A., Powell, K. A., Kuehn, R. E., Young, S. A., Winker, D. M., Hostetler, C. A., Hunt, W. H., Liu, Z. Y., McGill, M. J., and Getzewich, B. J.: Fully automated detection of cloud

ACPD
13, 14749–14795, 2013

and aerosol layers in the CALIPSO lidar measurements, J. Atmos. Ocean. Tech., 26, 2034–2050, doi:10.1175/2009jtecha1228.1, 2009.
Wandinger, U., Tesche, M., Seifert, P., Ansmann, A., Müller, D., and Althausen, D.: Size matters: Influence of multiple scattering on CALIPSO light-extinction profiling in desert dust, Geophys. Res. Lett., 37, L10801, doi:10.1029/2010GL042815, 2010.
Winker, D. M., Vaughan, M. A., Omar, A., Hu, Y., Powell, K. A., Liu, Z., Hunt, W. H., and Young, S. A.: Overview of the CALIPSO mission and CALIOP data processing algorithms, J. Atmos. Ocean. Tech., 26, 2310–2323, doi:10.1175/2009JTECHA1281.1, 2009.
Winker, D. M., Tackett, J. L., Getzewich, B. J., Liu, Z., Vaughan, M. A., and Rogers, R. R.: The global 3-D distribution of tropospheric aerosols as characterized by CALIOP, Atmos. Chem. Phys., 13, 3345–3361, doi:10.5194/acp-13-3345-2013, 2013.
Young, S. A. and Vaughan, M. A.: The retrieval of profiles of particulate extinction from cloud-aerosol lidar infrared pathfinder satellite observations (CALIPSO) data: algorithm description, J. Atmos. Ocean. Tech., 26, 1105–1119, doi:10.1175/2008JTECHA1221.1, 2009.
Zhang, J. and Reid, J. S.: MODIS aerosol product analysis for data assimilation: assessment of over-ocean level 2 aerosol optical thickness retrievals, J. Geophys. Res., 111, D22207, doi:10.1029/2005JD006898, 2006.
Zhang, L., Gong, S., Padro, J., and Barrie, L.: A size-segregated particle dry deposition scheme for an atmospheric aerosol module, Atmos. Environ., 35, 549–560, doi:10.1016/S1352-2310(00)00326-5, 2001.
Zhang, J., Reid, J. S., and Holben, B. N.: An analysis of potential cloud artifacts in MODIS over ocean aerosol optical thickness products, Geophys. Res. Lett., 32, L15803, doi:10.1029/2005GL023254, 2005.

ACPD
13, 14749–14795, 2013

ACPD
13, 14749–14795, 2013

Table 1. Statistical indicators for CALIPSO and AERONET comparisons under different LR assumption for CALIOP (40 sr vs. 58 sr). Average CALIPSO aerosol optical depth at 532 nm (τ_C), absolute bias (B_a), absolute standard error (σ_a), student's t test score (t), p value (p), relative bias, (B_r), root-mean-square error (RMS), correlation coefficient (R_{fit}), slope (S_{fit}) and intercept (I_{fit}) of the linear fit and number of comparisons (N) are shown. Average AERONET aerosol optical depth at 532 nm for this dataset is 0.249.

LR (sr)	τ_C	B_a	σ_a	t	p	B_r	RMS	R_{fit}	S_{fit}	I_{fit}	N
40	0.156	−0.093	0.027	−3.461	0.001	−0.372	0.122	0.922	0.702	−0.018	85
58	0.219	−0.030	0.031	−0.977	0.329	−0.121	0.085	0.922	0.965	−0.022	85

Table 2. Statistical indicators for CALIPSO and MODIS comparisons under different LR assumption for CALIOP (40 sr vs. 58 sr). Average CALIPSO aerosol optical depth at 532 nm (τ_C), absolute bias (B_a), absolute standard error (σ_a), student's t test score (t), p value (p), relative bias (B_r), root-mean-square error (RMS), correlation coefficient (R_{fit}), slope (S_{fit}) and intercept (I_{fit}) of the linear fit and number of comparisons (N) are shown. Average MODIS aerosol optical depth at 532 nm for this dataset is 0.204.

LR (sr)	τ_C	B_a	σ_a	t	p	B_r	RMS	R_{fit}	S_{fit}	I_{fit}	N
40	0.106	−0.076	0.011	−6.597	1×10^{-10}	−0.334	0.108	0.738	0.704	−0.008	178
58	0.145	−0.019	0.014	−1.380	0.168	−0.083	0.099	0.738	0.970	−0.012	178

ACPD
13, 14749–14795, 2013

Optimizing Saharan dust CALIPSO retrievals

V. Amiridis et al.

Title Page
Abstract | Introduction
Conclusions | References
Tables | Figures
◀ | ▶
Back | Close
Full Screen / Esc
Printer-friendly Version
Interactive Discussion

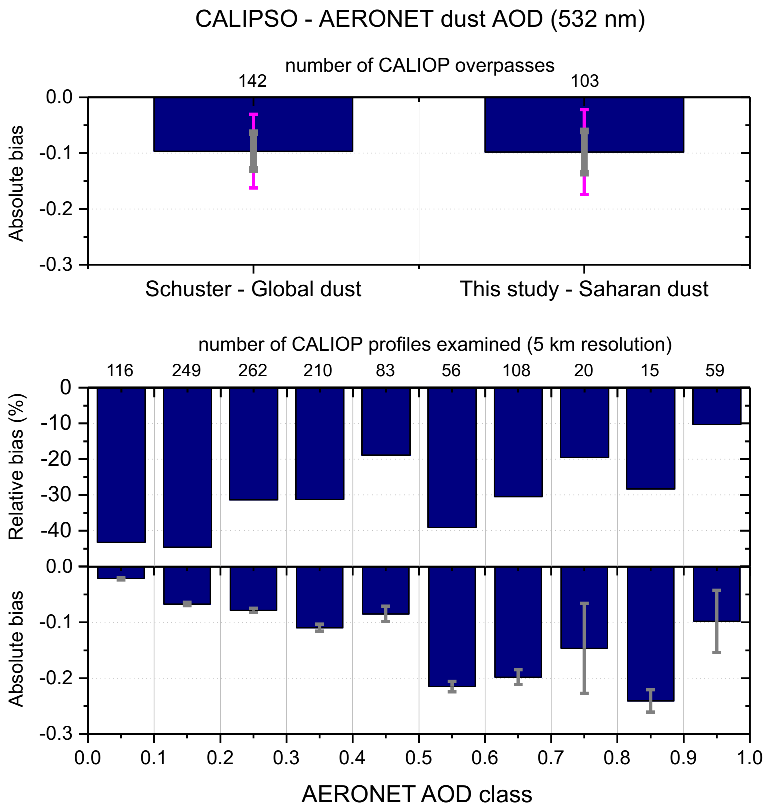

Fig. 1. Upper: mean absolute bias of CALIPSO – AERONET AODs from Schuster et al. (2012), for globe (left), and our dataset for Saharan dust (right). Lower: relative and absolute biases for our correlative dataset per AOD class.

ACPD
13, 14749–14795, 2013

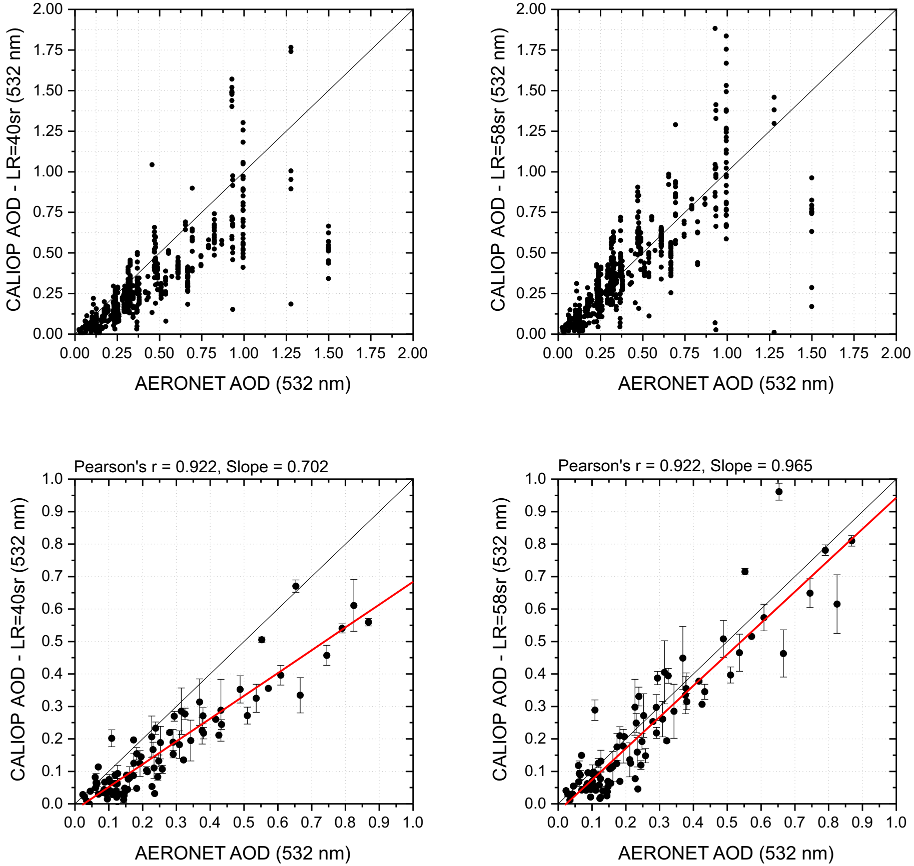

Fig. 2. Upper: scatter plot comparison of CALIPSO 5 km AOD versus collocated AERONET measurements when LR is equal to 40 sr (left) and when LR is equal to 58 sr (right). Lower: scatter plot comparison of CALIPSO averaged AODs versus collocated AERONET measurements, for spatially homogeneous coincidences in 80 km distance when LR is equal to 40 sr (left) and when LR is equal to 58 sr (right).

ACPD
13, 14749–14795, 2013

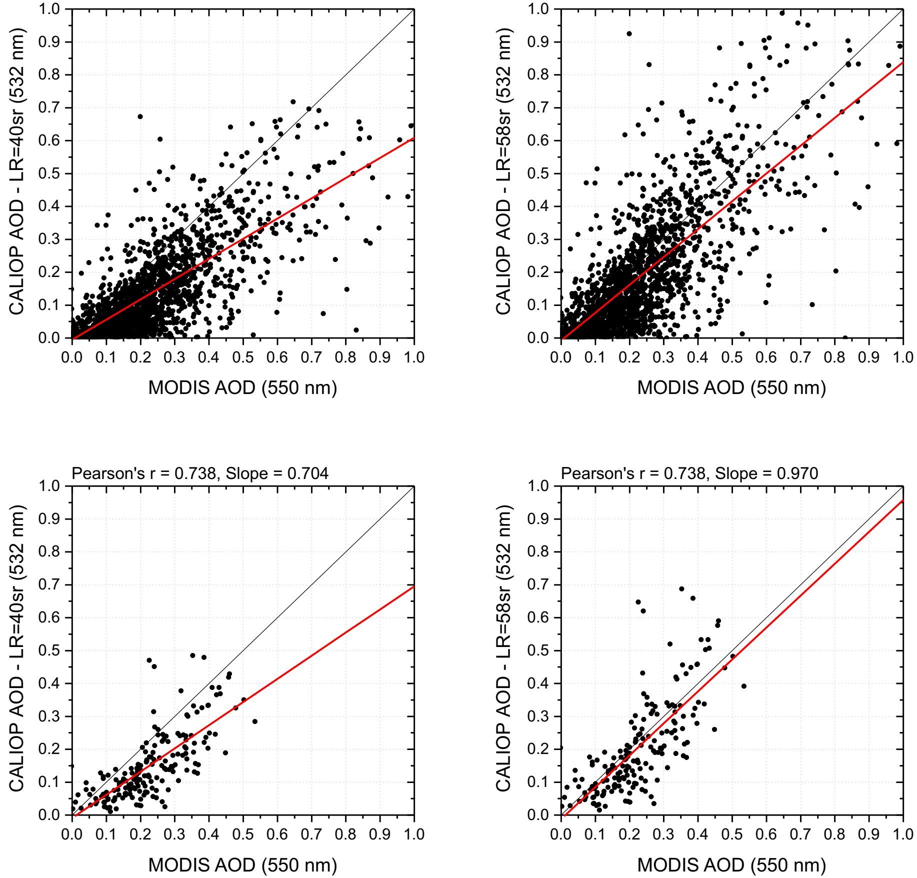

Fig. 3. Scatter plot comparison of CALIPSO spatial averaged AODs (1° × 1°) versus collocated MODIS-Aqual Level 3 cloud-free product. Upper: no filters applied for LR equal to 40 sr (left) and LR equal to 58 sr (right). Lower: filters for dust presence, cloudiness and MODIS sampling applied for LR equal to 40 sr (left) and LR equal to 58 sr (right).

ACPD
13, 14749–14795, 2013

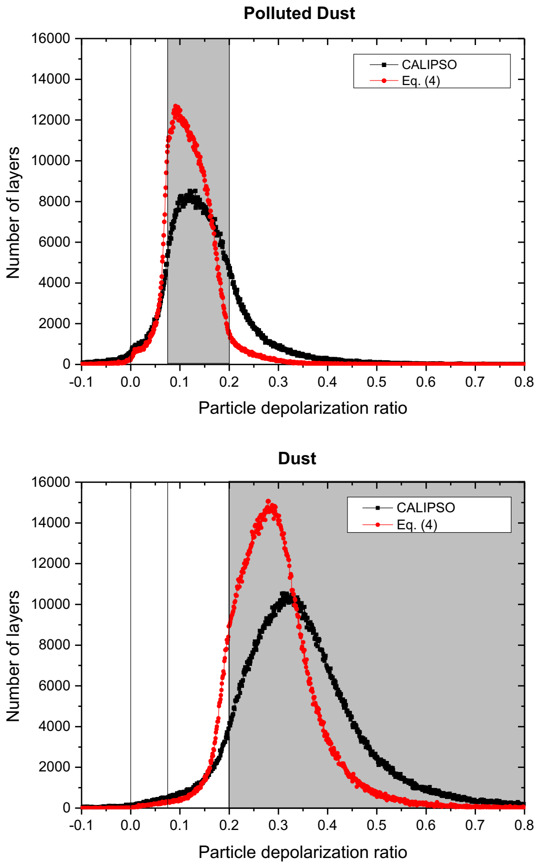

Fig. 4. Upper: particle depolarization ratio distributions for the Polluted Dust layers examined. Black curve represents the reported Level 2 product by CALIPSO and red curve represents the re-calculated values using perpendicular and total backscatter product. Lower: the same as upper panel but for layers categorized as dust.

Discussion Paper | Discussion Paper | Discussion Paper | Discussion Paper |

ACPD

13, 14749–14795, 2013

Optimizing Saharan dust CALIPSO retrievals

V. Amiridis et al.

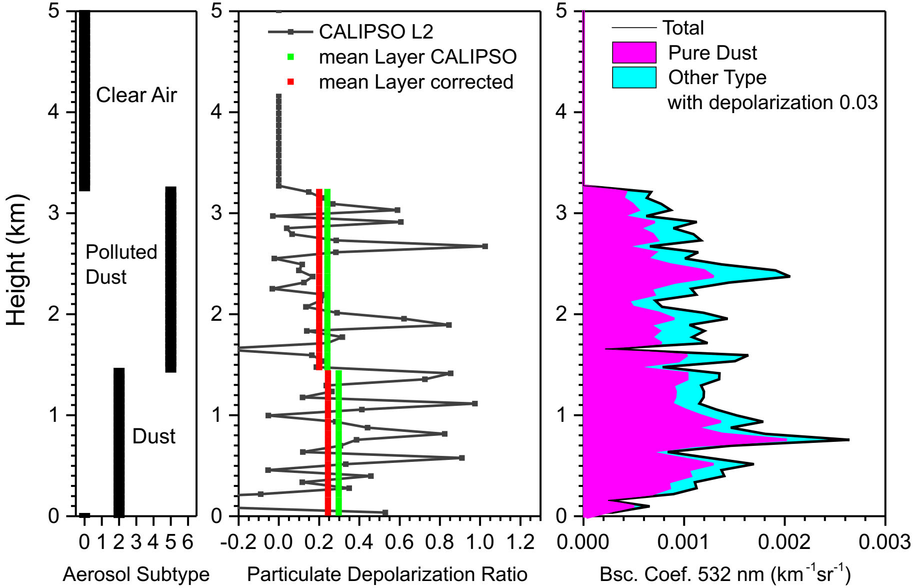

Fig. 5. Example of the application of Tesche et al. (2009) methodology for the discrimination of pure dust from dust mixtures. Left: aerosol type. Middle: particle depolarization ratio (black line), mean layer depolarization reported by CALIPSO (red line) and mean particle depolarization ratio re-calculated by the mean layer total and perpendicular backscatter coefficients (green line). Right: backscatter coefficient separation for pure dust (in magenta color) and "other" aerosol type (in cyan color).

ACPD
13, 14749–14795, 2013

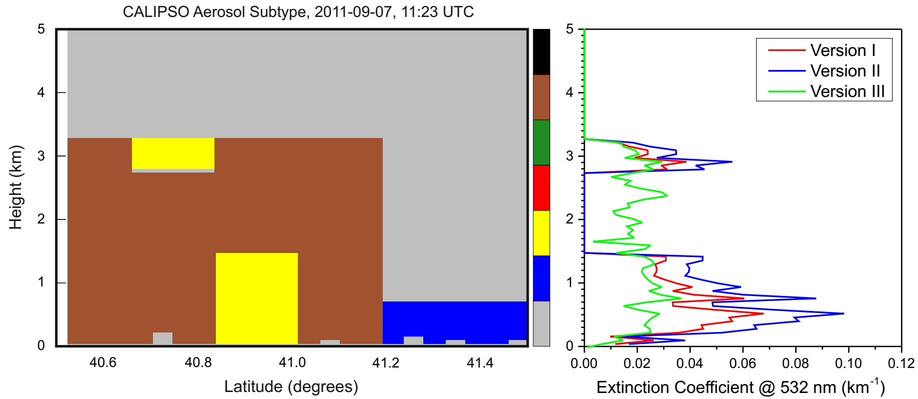

Fig. 6. Example of the averaging procedure followed for the three different Versions of CALIPSO climatological products for 7 September 2011 at 11:23 UTC. Left panel shows the CALIPSO aerosol subtype: clean marine (blue), dust (yellow), polluted continental (red), clean continental (green), polluted dust (brown) and smoke (black). Right panel presents the corresponding averaged extinction coefficient profiles at 532 nm following the three different Versions of CALIPSO climatological product.

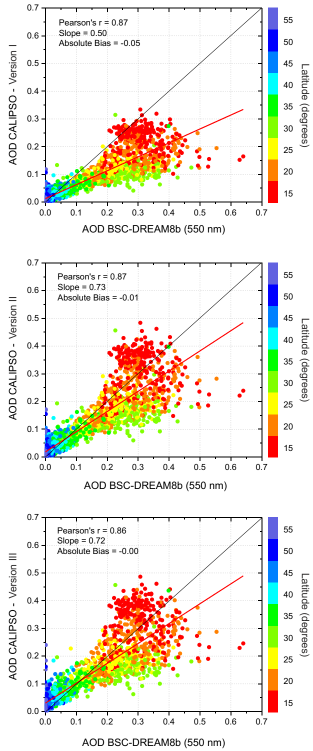

Fig. 7. Comparison of CALIPSO and BSC-DREAM8b dust AODs for (upper) original Version I CALIPSO AODs, (middle) Version II CALIPSO AODs for LR equal to 58 sr, (lower) Version III CALIPSO AODs for LR equal to 58 sr and acknowledgment of non-dust aerosol types (extinction equal to zero) in the averaging scheme as well as pure dust component contained in dust and polluted dust types. Color bar represents the latitudinal zone of the comparison, in 5 degree bins.

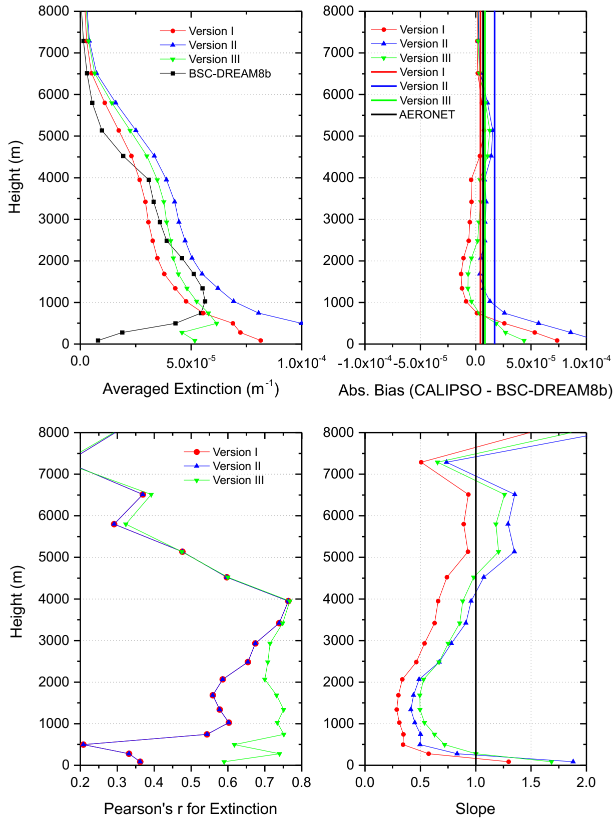

Fig. 8. Comparison between Level 3 extinction CALIPSO product and BSC-DREAM8b model outputs for the three Versions of CALIPSO climatological product. Upper: averaged extinction profile over the domain (left) and absolute biases (right). Lower: Pearson's correlation coefficient profile for the domain (left) and regression slopes (right).

ACPD
13, 14749–14795, 2013

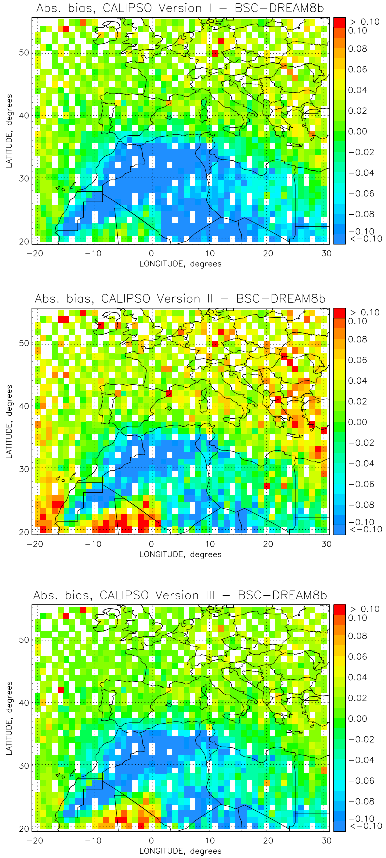

Fig. 9. Spatial distribution of 5 yr AOD absolute biases for the three Versions of CALIPSO climatological product and the BSC-DREAM8b dust model outputs.

ACPD
13, 14749–14795, 2013

Optimizing Saharan dust CALIPSO retrievals

V. Amiridis et al.

Title Page
Abstract | Introduction
Conclusions | References
Tables | Figures
◄| |►
◄ ►
Back | Close
Full Screen / Esc
Printer-friendly Version
Interactive Discussion

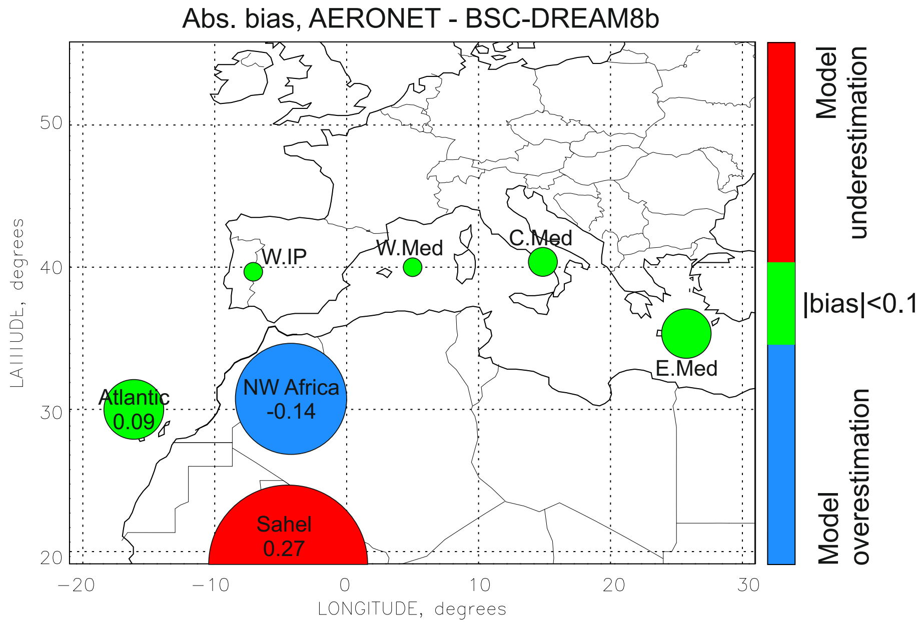

Fig. 10. Spatial distribution of AOD model absolute biases from the BSC-DREAM8b evaluation against AERONET (Basart et al., 2012).

ACPD
13, 14749–14795, 2013